Regularization of dynamics in an ensemble of nondiffusively coupled chaotic elements

A. S. Kuznetsov*
Center for BioDynamics and Mathematics Department, Boston University, 111 Cummington St., Boston, Massachusetts 02215, USA and Department of Mathematical Sciences, Indiana University Purdue University Indianapolis, Indianapolis, Indiana 46202, USA§

V. D. Shalfeev†
Radiophysics Department, Nizhni Novgorod University, Gagarin Avenue 23, 603950, Nizhni Novgorod, Russia

L. S. Tsimring‡
Institute for Nonlinear Science, University of California, San Diego, La Jolla, California 92093-0402, USA
(Received 11 January 2005; revised manuscript received 14 July 2005; published 17 October 2005)

We investigate the dynamics in an ensemble of chaotic elements with nondiffusive coupling. First, we analyze the case of global coupling. The type of coupling we consider leads to the suppression of oscillations in the whole ensemble at a high coupling strength. A distinct feature of this transition from high-dimensional chaos at a low coupling strength to the stationary state is that there is no partially ordered phase characterized by a large number of coexisting synchronized clusters. A two-cluster mode emerges abruptly, replacing the asynchronous mode. We focus on the influence of connectivity on the dynamics in the two-cluster modes and their domains of existence. We introduce a parameter that characterizes the connectivity: the range of coupling. Our computational and analytical results indicate that the most significant changes in the dynamics occur in the case of local coupling, when extra connections are added. By contrast, if the range of coupling is high, even substantial changes in this range have a small influence on the dynamics.

DOI: 10.1103/PhysRevE.72.046209 PACS number(s): 05.45.Xt, 89.75.Kd, 82.40.Bj

I. INTRODUCTION

Mechanisms of transition between chaotic and regular collective dynamics in ensembles of coupled elements has been a subject of intensive study nowadays (see, e.g., Ref. [1], and references therein). Chaotic collective dynamics may emerge in ensembles of simple oscillators with amplitude-dependent frequencies or when their natural frequencies differ [2–6]. In ensembles of chaotic elements, collective chaos emerges from the dynamics of individual elements and does not require the ensemble to be nonhomogeneous. However, in both cases, the chaoticity of the dynamics may be reduced or entirely suppressed when the coupling strength increases [2–10]. The mechanisms and properties of such a regularization transition vary significantly from system to system.

Spontaneously emerging synchronous clusters are known to accompany this regularization [7–11]. In an ensemble of simplest identical phase oscillators, formation of clusters can be achieved when a multiharmonic coupling function is considered [12]. In a more complicated ensemble of globally coupled chaotic maps, the transition between a turbulent phase and a completely synchronous state occurs through a partially ordered phase, where a wide variety of clusters coexists, and an ordered phase, where there are only a few clusters [7]. So, when the coupling increases, a gradual decrease in the number of the coexisting clusters eventually leads to the complete synchrony. A similar transitional cluster formation has been observed in a system of globally coupled Rössler oscillators, but the number of clusters was a strongly nonmonotonic function of the coupling strength [8]. The emergence of coherent clusters (elements of which are not exactly synchronized) was shown in a lattice of locally interacting Hindmarsh-Rose chaotic oscillators, which models biological excitable media [9]. There, the regularization mechanism was shown to be related to the appearance of periodic dynamics in a local analog of the mean field for a group of neurons. In Ref. [10], the transitional clusterization has been observed experimentally: when global coupling was applied to an ensemble of chaotic electrochemical oscillators to achieve synchrony, stable clusters formed at an intermediate coupling strength.

The majority of studies and, in particular, all the papers mentioned above, focused on either global (all-to-all) or local diffusive-type coupling. These two cases are qualitatively different: in contrast to the local coupling, in globally coupled systems, there is no convergence toward statistical equilibrium, i.e., the variance of the mean field does not depend on the number of elements N as $1/N$, but reaches saturation for large N [13,14]. It is very interesting to study systematically the variation in properties of an ensemble when the connectivity continuously varies between local and global. This area of research has become very active in the last several years. A desynchronization transition in an ensemble of phase oscillators [15] and sine-circle maps [16] has been observed as the range of interactions decreases. The synchronization of a one-dimensional array of phase oscillators with purely repulsive (inhibitory) coupling of varying range was recently studied in Ref. [17], showing a surprising

*Electronic address: akuznetsov@math.iupui.edu
†Electronic address: shalfeev@rf.unn.ru
‡Electronic address: ltsimring@ucsd.edu
§Present address.

advantage of the local coupling in synchronizing the array. Another result for phase oscillators [18] and for chaotic maps [19] with long-range interactions indicate the dependence of the synchronization on the number of dimensions of the array. An interesting dependence of the length of a transient on the network connectivity is shown for pulse-coupled oscillators in Ref. [20]. In Ref. [21], the authors have shown that the degree of connectivity in an ensemble of randomly coupled chaotic maps is critical for formation of clusters. Finally, in a recent paper [22] the authors studied pattern formation in a two-dimensional array of phase oscillators with varying range of phase-shifted coupling.

In this paper, we study an ensemble of oscillators with frequency control [23] frequency locked loop (FLL) and phase locked loop (PLL), which are widely used as a model for various technological systems such as phase antenna arrays [24,25], digital data transmission systems [26,27], laser frequency control [28], and superprecise measurements [29,30]. What makes this system different from more commonly studied models is a strongly nonlinear, nondiffusive type of coupling. This type of coupling emerges naturally in technological applications (PLLs and FLLs). In addition growing interest in nonlinear nondiffusive coupling is also motivated by its relevance in neurobiology, where various types of synaptic coupling (both inhibitory and excitatory) are prevalent [31]. Each oscillator in our ensemble is described as a three-dimensional system of ODE, and in isolation it displays chaotic dynamics. Our study shows that, if the coupling is sufficiently strong, then a uniform stationary state is realized in the system. Thus, the introduction of the nonlinear nondiffusive coupling between the elements leads to a transition from chaotic to regular oscillations and, eventually, to the suppression of the latter. A distinct feature of the transition from the high-dimensional chaos at a low coupling strength to the stationary state is that there is no partially ordered phase with a rich variety of coexisting cluster modes. A two-cluster mode emerges abruptly, replacing the asynchronous mode.

We focus on the investigation of the influence of connectivity on the dynamics for the two-cluster solutions and their domains of existence. We introduce a parameter that characterizes the connectivity: the range of coupling. When the range of coupling S decreases, the existence domains of the two-cluster modes shrink. We distinguish a common feature of our diagrams: almost all of the cluster modes do not exist in the case of local coupling $S=1$. But, by contrast, all these modes have significant existence domains at $S \geqslant 2$. This means that the boundaries of the existence domains undergo a very sharp transition when the range of coupling S changes from 1 to 2. This result is also supported by our analytic calculations of the stability boundary for the homogeneous passive mode (stationary state), which shows the most significant shift when S changes from 1 to 2.

The paper is organized as follows. In Sec. II we present the model for the individual chaotic oscillator and nonlinear coupling and briefly discuss their properties. Section III is devoted to the case of globally coupled ensemble. Here we introduce and investigate the two-cluster reduced model describing the partially synchronized state of the ensemble. We also study the stability properties of homogeneous states in this section. In Sec. IV we investigate the influence of variable connectivity on the dynamics of coupled chaotic elements. Section V presents our conclusions.

II. MODEL

We take the following set of equations as a mathematical model for the isolated element of the ensemble [32]:

$$\frac{dx}{dt} = \alpha[y - x + f(x)],$$

$$\frac{dy}{dt} = x - y + z,$$

$$\frac{dz}{dt} = -\beta y. \tag{1}$$

Here, α and β are positive parameters. We choose a smooth function in the form

$$f(x) = \frac{2c_0 x}{1 + c_0^2 x^2} - c_1 x^3, \tag{2}$$

where c_1 is small, to describe the nonlinearity of the element. Equations (1) describe an electronic circuit known as Chua's circuit [33]. In this case, the variables represent dimensionless currents and voltages. On the other hand, the equation for an oscillator with frequency control [23] reduces to the system (1) in a certain case. Then, the variable x represents relative deviation of the oscillator frequency from the reference frequency and $f(x)$ is the nonlinear characteristic of the frequency discriminator in the control loop. In this paper, we focus on the latter application.

Now we introduce the model of an ensemble in which by varying a parameter it is possible to pass from a chain of locally coupled elements to an ensemble with global coupling. Each element in this chain is coupled with S right-side and S left-side neighboring elements:

$$\frac{dx_i}{dt} = \alpha[y_i - x_i + f(x_i)] + \frac{d}{2S}\sum_{k=1}^{S}[F(x_{i-k}) + F(x_{i+k})],$$

$$\frac{dy_i}{dt} = x_i - y_i + z_i,$$

$$\frac{dz_i}{dt} = -\beta y_i. \tag{3}$$

Here, i is the number of the element, $i = \overline{1,N}$, N is the number of elements in the ensemble, and d is the coupling parameter. We choose $N=55$ for our numerical experiments and discuss variations of this number in the analytical part of our study.

As seen in Eq. (3), the coupling term has the nondiffusive character. This choice is motivated by the fact that the individual element represents the loop of frequency control used for generators of various nature. The exchange of the signals from the control loop is the simplest and the most

natural way of connecting this systems, and this provides the nondiffusive type of coupling introduced in Eq. (3). In this case, the inputs from different elements sum when the elements are synchronized, in contrast to diffusive coupling, for which the coupling term vanishes in synchrony. In particular, in the state of full synchronization [$x_i=x(t)$ for all i], the sum in Eq. (3) gives $2SF(x)$, and we compensate this summation dividing the coupling term by $2S$. The adopted normalization allows us to focus on more complex effects than the summation.

Driven by the application of the considered system as an oscillator with frequency control, we take the coupling function in the form

$$F(x) = \frac{2\gamma x}{1+\gamma^2 x^2}, \tag{4}$$

which is very similar to the nonlinear characteristic of the partial element $f(x)$. Taking $F(x)=f(x)$ would mean that the signal from the frequency discriminator of each element is directly used as coupling. In this paper, we allow this two functions to be different taking γ not equal to c_0. Technically this means that another frequency discriminator is used for the coupling. Dynamical motivation of this choice is that now we have a possibility to superimpose attractors in the individual elements with different parts of the coupling function. Generally speaking, this coupling function represents one of the simplest nonlinear coupling schemes, which makes its choice logical in order to extend the exploration of dynamics to the case of nonlinear coupling.

In our computer simulations, parameters of an isolated element are chosen in the existence domain of a spiral chaotic attractor $\alpha=6.4$, $\beta=10$, $c_0=0.7$, $c_1=0.05$. We assume periodic boundary conditions $x_{i-k}=x_{i-k+N}$ for all $i-k<1$; $x_{i+k}=x_{i+k-N}$ for all $i+k>N$. The global coupling corresponds to $S=(N-1)/2$. The other limiting case of the system (3), namely, a chain of locally coupled elements, is realized for $S=1$.

III. GLOBALLY COUPLED ENSEMBLE

In this section, we consider the globally coupled ensemble [$S=(N-1)/2$]. In this case, the sum that represents the influence of all the elements in the ensemble upon the ith element can be written as a sum of two parts:

$$\frac{1}{N-1}\sum_{j=1,j\neq i}^{N} F(x_j) = \frac{N}{N-1}B - \frac{1}{N-1}F(x_i), \tag{5}$$

where $B=(1/N)\Sigma_{j=1}^{N}F(x_j)$ is called a mean field, and the second part depends on x_i only. Thus, the elements of any ensemble with global coupling interact with each other only through the mean field, which renders the spatial organization of the array irrelevant.

A. Synchronization of elements in an ensemble with global coupling

First, we describe the changes in dynamics of the globally connected ensemble when the coupling coefficient is varied.

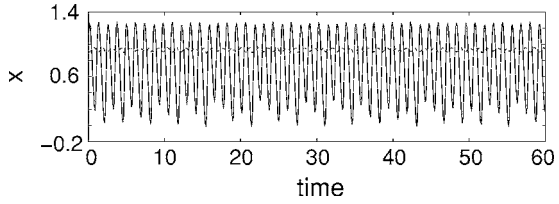

FIG. 1. A pair of clusters: $d=0.55$. The time series of the x variables for two elements that belong to different clusters. We call the element with large amplitude active, and with small passive.

An asynchronous mode of oscillations of elements is observed in computer simulations for small values of the coupling parameter. If the coupling parameter exceeds a bifurcation value, the asynchronous mode collapses, and one of synchronous modes sets in with formation of a pair of clusters so that some elements of the ensemble belong to one cluster, all the rest to the other cluster. Inside the clusters, the elements are synchronized in phase, so that

$$x_i = a_1(t), \quad y_i = b_1(t), \quad z_i = c_1(t); \quad i = \overline{1,M}, \tag{6}$$

$$x_j = a_2(t), \quad y_j = b_2(t), \quad z_j = c_2(t); \quad j = \overline{M+1,N}.$$

A variety of such two-cluster modes, which different from one another by the number of the elements belonging to one of the clusters, M, coexists, giving rise to multistability. Figure 1 presents the time series for the x variables of two elements that belong to different clusters. The difference between the amplitude of oscillations in these time-series allows us to refer to one of the clusters as active and the other as passive. Figure 2 shows the existence domain of these modes, denoted as D, depending on the coupling parameter and the number of elements belonging to the active cluster for $\gamma=3$. In the limiting cases, all N elements belong to one cluster. We call the mode homogeneous active if all elements are active, and homogeneous passive if all of them are passive. Note that the homogeneous passive mode is stationary, and its existence domain is not bounded from above, in contrast to all synchronous modes.

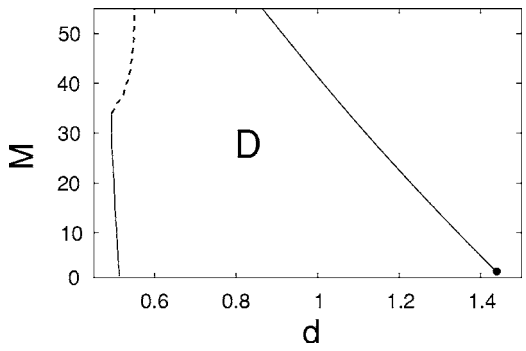

FIG. 2. The domain of existence of the two-cluster modes D vs the number of active elements M. The curve composed of the solid and dashed segments corresponds to the loss of transversal stability of the corresponding manifold. The dashed part is a fuzzy boundary (see an explanation below).

Thus, the introduction of the global coupling among the elements of the ensemble causes formation of a pair of clusters, within which all the elements are synchronized in phase. In contrast to other known cases, there is no transitional decrease in the number of clusters, i.e., with growing coupling strength, the pair of clusters emerges abruptly, replacing the asynchronous mode. In the existence domain of the cluster modes, the ensemble possesses high-order multistability, and the particular cluster mode that sets in depends on the initial conditions. Once a mode sets in, it preserves up to the coupling strength corresponding to the upper boundary of the existence domain of this mode. When the coupling strength exceeds the latter value, the number of elements in the passive cluster grows due to a transition to another cluster mode. This gradual growth of the passive cluster eventually leads to the collapse of oscillations and emergence of the homogeneous passive mode, which remains stable for arbitrary strong coupling.

B. Homogeneous passive mode

Now, we analyze homogeneous modes realized in the ensemble with global coupling. The equality of the corresponding variables of all elements holds:

$$x_j = x(t), \quad y_j = y(t), \quad z_j = z(t); \quad j = \overline{1,N}. \tag{7}$$

This condition describes the manifold of the homogeneous modes, where both active and passive modes are located. By substituting Eq. (7) into the system (3) in the case of global coupling [below denoted as Eq. $(3)_{\text{glob}}$], we obtain a reduced model for dynamics in the homogeneous modes:

$$\frac{dx}{dt} = \alpha(y - x + f(x)) + dF(x),$$

$$\frac{dy}{dt} = x - y + z,$$

$$\frac{dz}{dt} = -\beta y. \tag{8}$$

The homogeneous passive mode can be viewed as the limiting case of the cluster mode in which there are no active elements in the ensemble. The coordinates of the equilibrium state corresponding to this mode can be easily obtained from the system (8) as functions of the coupling parameter. The characteristic equation describing stability of this equilibrium state can be obtained analytically and splits into N equations in the form

$$[\sigma(x_0) - \lambda][\lambda^2 + \lambda + \beta] + \alpha\lambda = -d\Omega(n,x_0)[\lambda^2 + \lambda + \beta], \tag{9}$$

where $n = \overline{1,N}$, $\sigma(x_0) = \alpha[-1 + f_x'(x_0)]$, and x_0 is the x coordinate of the equilibrium state. The coefficient $\Omega(n,x_0)$ is written as

$$\Omega(n,x_0) = 2\frac{F_x'(x_0)}{N-1}\sum_{k=1}^{N/2-1}\cos\left(\frac{2\pi kn}{N}\right) + \cos(\pi n), \tag{10}$$

for an even number of elements N, and as

$$\Omega(n,x_0) = 2\frac{F_x'(x_0)}{N-1}\sum_{k=1}^{(N-1)/2}\cos\left(\frac{2\pi kn}{N}\right) \tag{11}$$

for an odd number of elements. In both cases, it is easy to obtain

$$\Omega(n,x_0) = \begin{cases} F_x'(x_0) & \text{if } n = N, \\ -\dfrac{F_x'(x_0)}{N-1} & \text{if } n \neq N. \end{cases} \tag{12}$$

Hence, one of the N equations has a form

$$[\sigma(x_0) - \lambda][\lambda^2 + \lambda + \beta] + \alpha\lambda = -dF_x'(x_0)[\lambda^2 + \lambda + \beta], \tag{13}$$

and all the rest are written as

$$[\sigma(x_0) - \lambda][\lambda^2 + \lambda + \beta] + \alpha\lambda = \frac{d}{N-1}F_x'(x_0)[\lambda^2 + \lambda + \beta]. \tag{14}$$

Both of these equations are third-order with respect to λ. Writing the above equations in the general form $\lambda^3 + a\lambda^2 + b\lambda + c = 0$ and using the standard criteria under which a bifurcation of the birth of a limit cycle from an equilibrium state or contraction of a limit cycle to an equilibrium state $ab - c = 0$ occurs, we arrive at the equation

$$d\Omega(n,x_0) = -\sigma(x_0) + \frac{1 - \alpha \pm \sqrt{1 + \alpha^2 + 2\alpha - 4\beta}}{2}. \tag{15}$$

The substitution of the values (12) for $\Omega(n,x_0)$ yields equations for two curves in the space of parameters. On one of these curves, a single bifurcation of the birth of a saddle limit cycle from the equilibrium state occurs. On the other one, $N-1$ such bifurcations occur simultaneously. The latter corresponds to a change in stability of the manifold of the homogeneous modes at the stationary state with respect to perturbations transversal to the manifold. The simultaneous occurrence of $N-1$ such bifurcations reflects the spacial degeneration of the system due to the global character of coupling. The single separate bifurcation corresponds to a change in stability of the equilibrium state inside the manifold of the homogeneous modes.

The order in which these two bifurcation points are arranged when d decreases depends on the parameter γ of the coupling function. As shown in Fig. 3, if γ is large, then the equilibrium state becomes stable with respect to all perturbations inside the manifold of the homogeneous modes first, and the consequent degenerate bifurcation giving the transversal stability determines the boundary of its stability domain. In contrast, if γ is small, the order of these bifurcations is reversed. It is obvious that these two curves intersect at the point that corresponds to $F_x'(x_0) = 0$ because $\Omega(n,x_0) = 0$ at this point, and Eqs. (13) and (14) become identical. Due to the opposite signs in front of the right-hand sides (RHSs) of these equations, the direction of the shift for the bifurcation points, when $F_x'(x_0) \neq 0$ is introduced, must be opposite, but which of them occurs at a lower coupling strength depends on the sign of $F_x'(x_0)$. In our case, for lower γ, $F_x'(x_0) > 0$,

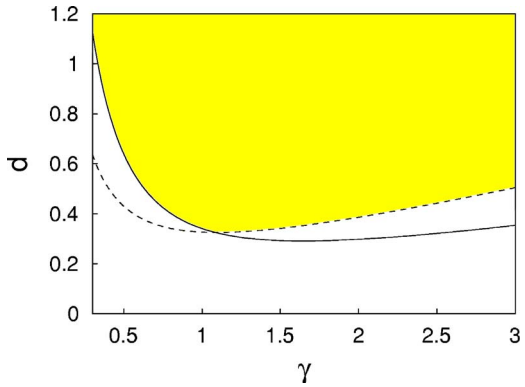

FIG. 3. (Color online) Bifurcation boundaries for the equilibrium state for the homogeneous passive mode [Eq. (15)]. The solid curve corresponds to the single separate bifurcation inside the manifold [see Eq. (13)]. The dashed curve shows the degenerate bifurcation that changes the transversal stability of the manifold at the equilibrium [see Eq. (14)].

which introduces a dissipative term into the system for transversal perturbations (see Appendix) and shifts the corresponding bifurcation boundary downward with respect to the coupling strength. Simultaneously, a term that can be interpreted as negative effective dissipation (the coupling term) is introduced into the system (8), stability analysis of which gives Eq. (13). Consequently, the point of the bifurcation inside the manifold shifts upward. Similar reasoning can be applied to the case $F_x'(x_0)<0$. Thus, the order of the bifurcations is determined by the sign of the first derivative of the coupling function.

What also makes the RHS of Eq. (14) [but not Eq. (13)] to vanish is growing number of elements N. The stability boundary as a function of N is shown in Fig. 4. In the limit $N\to\infty$, the system for transversal perturbations (Appendix) coincides with the linearized system for the element in isolation (1), and consequently Eq. (14) takes the form of the characteristic equation for the isolated element. For large N,

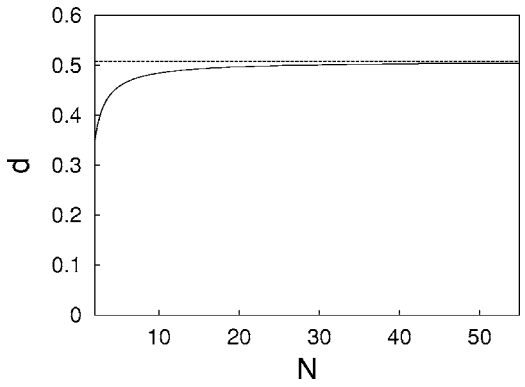

FIG. 4. The boundary (15) of the stability domain of the equilibrium state as a function of the number of elements in the ensemble N in the case $\gamma=3$. The dashed line shows asymptotes for $N\to\infty$, calculated when the RHS of Eq. (14) is zero. In the case of low γ, the boundary does not depend on N because it is determined by a bifurcation inside the manifold of the homogeneous modes (data not shown).

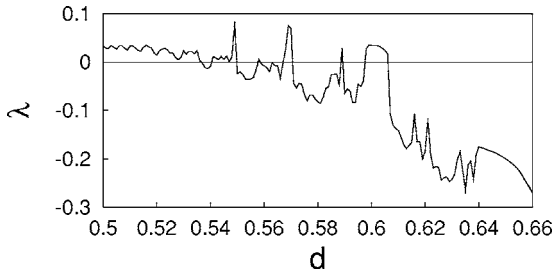

FIG. 5. The maximal transversal Lyapunov exponent for the homogeneous active mode at the lower boundary of its existence domain. The mode is stable where the exponent is negative.

neither the dynamics on the manifold, driven by Eq. (8), nor the transversal stability depends on N, leading to a horizontal asymptotes of $d(N)$. We note that the adopted normalization of the coupling by $1/(N-1)$ contributes to this effect because it eliminates N in system (8). We also note that, for the case of large number of elements, the transversal stability is affected by the coupling indirectly only, i.e., due to changes in dynamics and shifts of the attractor on the manifold.

C. Homogeneous active mode

The dynamics in the homogeneous active (oscillatory) mode is much more complex. At the lower boundary of its existence domain, it is chaotic. As the coupling strength d increases, a reverse Feigenbaum scheme (period halving) is realized inside the domain. This way the system transits from chaotic to regular dynamics. Obviously, this transition can be described in the framework of the reduced system (8) because synchrony does not violate. In contrast to the homogeneous passive mode, the existence domain for the active one is bounded from above. Our investigation shows that this boundary exists in the reduced system (8) as well, but it may not coincide with the upper boundary for the domain for this mode in the full system $(3)_{\text{glob}}$, which may occur at a lower coupling strength.

The chaoticity of the dynamics leads to a very complex structure of the lower boundary of the existence domain for the homogeneous active mode. Figure 5 presents the maximal transversal Lyapunov exponent for the system in this mode. When the exponent is negative, it shows stability with respect to the transversal perturbations. As the coupling parameter increases, the exponent crosses zero several times in a short interval, indicating that the mode becomes stable and then unstable repeatedly. We note that the stability loss is associated with emergence of periodic windows and some other structural changes of the attractor.

Figure 6 shows the existence domain of the homogeneous active mode as a function of γ. The mode is stable for no coupling strength when γ is small. For a high γ, the lower boundary of the domain is fuzzy because of chaoticity of the attractor, as described above. We depict the points at which the transverse Lyapunov exponent is equal zero. For higher coupling strength, the mode remains stable up to the saddle-node bifurcation of the limit cycle, as a result of which the mode collapses. By contrast, for lower γ, there is a loss of transversal stability at a coupling strength lower than the

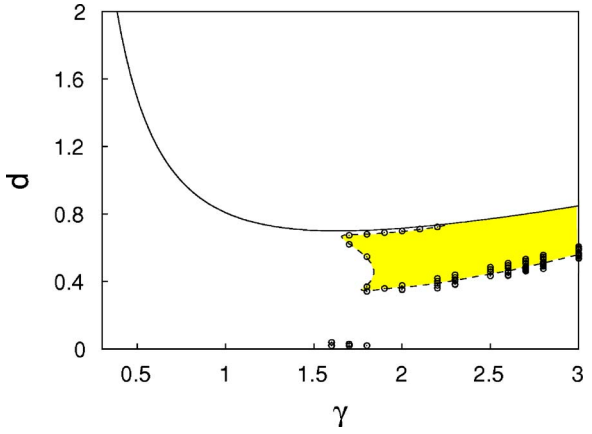

FIG. 6. (Color online) The boundaries of the existence domain of the homogeneous active mode as a function of γ. The solid curve corresponds to the saddle-node bifurcation of the limit cycle corresponding to the mode. The dashed curve is a schematic curve of the loss of the transversal stability (synchronization threshold), which is fuzzy. The real points where the mode changes its transversal stability are shown by circles.

saddle-node bifurcation (see, e.g., $\gamma=2$). Moreover, the stability domain splits into a few well separated intervals of d (as for $\gamma=1.8$). We sketch the synchronization threshold (the boundary of loss of the transversal stability) by the dashed curve, keeping in mind that it corresponds to a set of very close bifurcation curves.

D. Two-cluster modes

Next, we analyze the dynamics of the two-cluster modes, defined by Eq. (6). The latter condition gives us an invariant manifold for each number of active elements, M. Inside such a manifold, the dynamics is given by a six-dimensional reduced model, which can be obtained similar to the previous case (8) by substituting Eq. (6) into Eq. $(3)_{\text{glob}}$. Our investigation shows that, even though the passive elements are present in the ensemble, the dynamics and parametric portrait remain qualitatively the same as in the homogeneous active mode. However, the values of the coupling parameter corresponding to the period-halving bifurcations in the Feigenbaum cascade vary when the passive elements emerge.

The boundaries for the existence domain of the cluster modes also depend on the size of the passive cluster. We take $\gamma=3$ for further study. The upper boundary, which corresponds to the same saddle-node bifurcation of limit cycles, shifts to higher value of the coupling strength when the number of active elements decreases as shown in Fig. 2. The lower boundary corresponds to the loss of the transversal stability of the corresponding manifold. Given two distinct clusters now, it is enough that the transversal perturbations grow in only one of them in order for the mode to become unstable. The maximum transversal Lyapunov exponents for each of the clusters, shown in Fig. 7, say which cluster loses stability. The figure shows that, for small number of active elements, the passive cluster loses its stability first, while for large number of active elements, the active cluster becomes

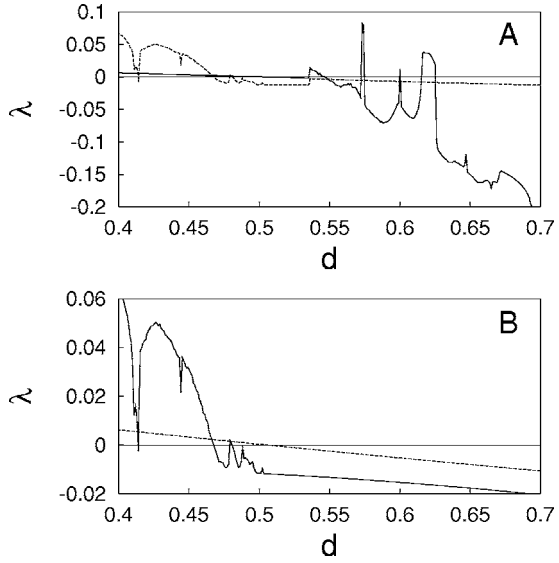

FIG. 7. The maximal transversal Lyapunov exponents as a function of the coupling strength for each of the clusters in a two-cluster mode. The solid curve corresponds to the active cluster, the dashed one to the passive. (A) $M=45$; (B) $M=10$.

unstable first. This perfectly agrees with the limiting cases of homogeneous modes. At an intermediate number of active elements, the synchronization threshold has a cusp that indicates the collision of these two scenario of the loss of synchrony.

IV. DYNAMICS OF THE ENSEMBLE WITH VARIABLE RANGE OF COUPLING

In this section, we study the changes in the dynamics of the system (3) when the range of coupling is varied.

A. Homogeneous modes

Consider first the effect of changing the connectivity on the homogeneous modes in the ensemble. As before, these modes are defined by the identity of all corresponding variables of the elements (7). Substituting these equations into the initial model (3), we find that the dynamics in these modes is described by the same system (8) for any range of coupling. Thus, if the solution corresponding to a homogeneous mode remains stable when the range of coupling changes, then the dynamics in this mode must be independent on the range of coupling because the latter does not enter the system (8).

In particular, the equilibrium state corresponding to the homogeneous passive mode stays at the same position when the range of coupling varies. As in the case of global coupling, the characteristic equation describing stability of this equilibrium state splits into N third-order equations of the same form (9) for an arbitrary range of coupling, but the function $\Omega(n,x_0)$ takes the form

$$\Omega(n,x_0)=\frac{1}{S}F_x'(x_0)\sum_{k=1}^{S}\cos\left(\frac{2\pi kn}{N}\right), \tag{16}$$

where x_0 is the x coordinate of the equilibrium state. Analogously to the previous case we obtain N curves in the param-

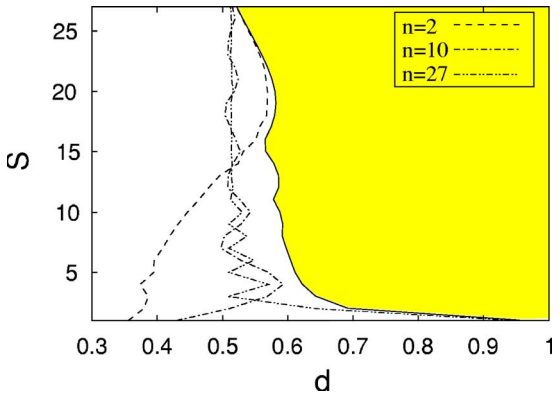

FIG. 8. (Color online) A few of the bifurcation curves (17) for the equilibrium state (dashed and dotted curves) corresponding to different $n(\gamma=3)$ vs the range of coupling S. The resulting stability domain of the equilibrium is shadowed and bounded by the solid curve.

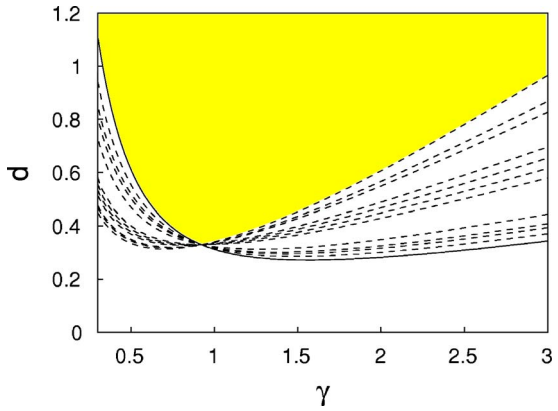

FIG. 9. (Color online) The bifurcation curves for the equilibrium state (17) in the case of local coupling. The solid curve coincides with that for global coupling.

eter space, on each of which a bifurcation of the birth of a saddle limit cycle from the equilibrium state occurs:

$$d^2\Omega(n)^2 + d\Omega(n)[2\sigma - 1 + \alpha] + [\beta - \sigma - \alpha + \sigma^2 + \sigma\alpha] = 0, \tag{17}$$

where $n=\overline{1,N}$.

The position of the bifurcation point corresponding to $n=N$ does not depend on the range of coupling, S, since $\Omega(N,x_0)=F_x'(x_0)$. Figure 8 presents a few of the bifurcation curves corresponding to different n and the stability domain of the equilibrium as a function of the range of coupling for $\gamma=3$. The curves converge to one point at $S=(N-1)/2$, which is the case of global coupling. When the coupling parameter increases, the stability of the equilibrium state is achieved only after all N bifurcations. When S varies, all these curves behave nonmonotonically and intersect, i.e., the order of these bifurcations changes. Hence, the stability boundary is composed of segments of the bifurcation curves corresponding to different n. The most interesting fact is that the most significant shift of the boundary occurs in the interval where the range of coupling is very small, i.e., when it changes between 1 and 2.

Consider now the dependence of the bifurcation values and the boundary of the stability domain as a function of γ in the case of nonglobal coupling. As we said before, the bifurcation value corresponding to $n=N$ does not depend on the range of coupling. This is the bifurcation that occurs inside the manifold of the homogeneous modes, and its dependence on γ in the case of global coupling was given by the solid curve in Fig. 3. Hence, the same curve preserves for any coupling range. The other curve in Fig. 3 splits into $N-1$ bifurcation curves since the spacial degeneration is removed for nonglobal coupling. The splitting is maximal in the case of local coupling $S=1$, which is presented in Fig. 9, but the picture is qualitatively the same in other cases also. The figure shows that the solid curve, corresponding to $n=N$, bounds the other curves from below for high γ and from above for low γ. This means that the stability boundary of the equilibrium state does not depend on the range of coupling if γ is small because the boundary is determined by the bifurcation inside the manifold of the homogeneous modes, corresponds to $n=N$. By contrast, for high γ, the stability domain shows the dependence on S as in Fig. 8.

The solution corresponding to the homogeneous *active* mode also exists for changing range of coupling. Our computer experiments for $\gamma=3$ show that this mode remains stable when the range of coupling S decreases from global, and the dynamics in this mode does not depend on S, in complete agreement with the model (8). We have shown that when the range of coupling is decreased, the coupling parameter that corresponds to the upper boundary of the existence domain does not change. Hence, for any range of coupling, this bifurcation occurs inside the manifold of the homogeneous modes and is described by the reduced model (8).

But the uniform state (7) may become unstable, and so the lower boundary of the existence domain for this mode may change when the range of coupling varies. As before for global coupling, the lower boundary is fuzzy and showed schematically in Fig. 10 with an error $\delta d=0.1$. We note that at $S=1$ the mode does not exist for any value of the coupling parameter. In contrast to that, at $S=2$, the domain of its existence is $0.65 \lesssim d \lesssim 0.864$. The homogeneous mode collapses in the transition from $S=2$ to $S=1$ for an arbitrary values of the coupling parameter in the above interval. The

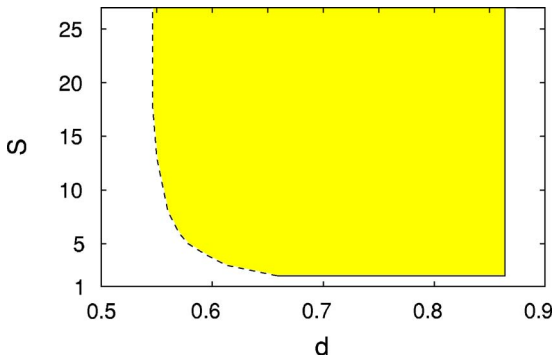

FIG. 10. (Color online) The existence domain of the homogeneous active mode vs the range of coupling S.

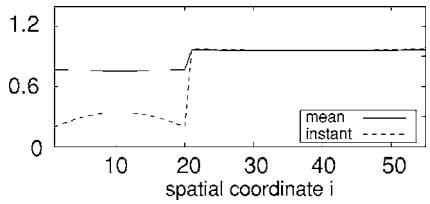

FIG. 11. The spatial distributions of the mean and the instantaneous values of x_i for an intermediate coupling range $S=9$.

fact that no changes occur in the reduced model (8) as a result of this transition indicates that an increase of the range of coupling causes loss of synchronization, i.e., loss of stability for the uniform distribution of variables. Consequently, the absence of the active homogeneous mode at $S=1$ (i.e., in the case of local coupling) is caused by a sharp increase in the value of the synchronization threshold. We described an analogous feature for the stability boundary of the homogeneous passive mode.

B. Pair of clusters

Next, we analyze the dependence of the two-cluster modes and their existence domains on the range of coupling in the ensemble. By contrast to the homogeneous mode, decreasing range of coupling changes the dynamics in the cluster modes: the dynamics of an element becomes dependent on its position relative to the boundary of the cluster. To illustrate that, we choose the cluster mode in which 20 neighboring elements constitute the active cluster, specify the coupling parameter $d=0.8$ and change the range of coupling from $S=(N-1)/2=27$ (global) to 1 (local). When the range of coupling decreases, the ensemble acquires the spatial structure of a circular chain. Spatial distributions of instantaneous and average values of the x_i variables along the chain are plotted in Fig. 11 for an intermediate value of S. Apparently, the instantaneous and the mean values for the elements in the same cluster become nonidentical when S decreases. When the range of coupling decreases, the sag in the instantaneous distribution increases, indicating growing phase shifts between elements. However, for arbitrary range of coupling, it is possible to unambiguously classify the elements as active and passive by the difference in values of the mean variables. This allows us to define the boundaries of the existence domain for the modes, even though the type of synchronization is more complex when the coupling is not global, and the low-dimensional model (8), obviously, is not valid. However, when the coupling strength increases inside the existence domain for a two-cluster mode, the bifurcation transitions are the same as in the model (8): the modes are chaotic at a lower coupling strength and become periodic by the reverse Feigenbaum scheme.

Consider the dependence of the existence domains for the two-cluster modes on the range of coupling and the size of the active cluster. Figure 12 presents the boundaries for the domains of existence in the cases when the active cluster consists of 10, 20, 30, 40, and 50 neighboring elements. The comparison of the lower boundary for $M=10$ (the boldest solid curve) with the stability boundary for the homogeneous

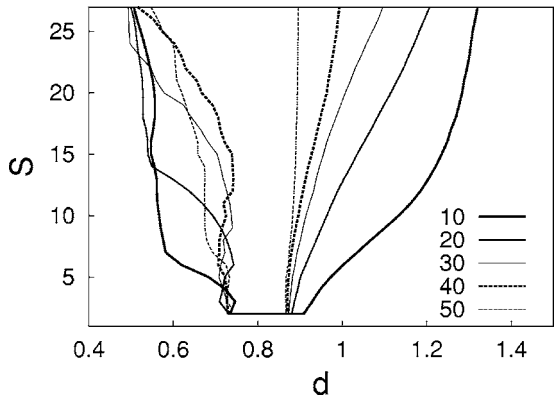

FIG. 12. The existence domains for the cluster modes composed of different number of elements. The number of active elements M corresponding to each of the curves is shown in the picture. (The fuzziness of the lower boundary is not reflected but persists in the majority of the cases.)

passive mode (see Fig. 8) shows that when the range of coupling is sufficiently large, these curves remain close and demonstrate a similar dependence on S. This dependence of the lower boundary for this cluster mode remains weak until $S=7$. When S decreases further, the coupling parameter at the boundary increases quickly from 0.5 to 0.74, and stays approximately at this value until $S=2$. The coupling parameter that corresponds to the upper boundary of the existence domain of this two-cluster mode shows a gradual monotonic decrease when the range of coupling S decreases. As a result, for $S=2$, the existence domain for the mode is approximately $0.74 \leqslant d \leqslant 0.91$. By contrast, this cluster mode does not exist in the local coupling case $S=1$. Thus, analogously to the homogeneous active mode, considered above, this two-cluster mode collapses in the transition from $S=2$ to $S=1$ in a long interval of the coupling parameter.

For low enough number of active elements ($M=20,30$), the lower boundary of the existence domain remains similar to one described above: when the range of coupling decreases, first, the coupling strength corresponding to the boundary shows a weak dependence on this parameter, but then undergoes a much sharper increase up to $d \approx 0.74$. The boundary stays approximately at this coupling strength till $S=2$. Comparing these graphs, we see that, as the number of active elements increases, the region of the weak dependence shrinks. In particular, for $M=20$, it ends at $S=14$, and, for $M=30$, at $S=24$. The boundary transits to $d \approx 0.74$ more gradually and stays at this value of the coupling parameter for a longer interval of the range of coupling, S. The changes are more pronounced when the number of active elements is greater (see dashed curves). Eventually, for $M=50$, both regions of weak dependence disappear, and the boundary displays a gradual shift to higher values of the coupling strength when the range of coupling decreases.

The upper boundary of the existence domains shows a gradual, monotonic dependence on the range of coupling in all of the considered cases. At $S=27$, i.e., in the case of global coupling, there is a significant difference in the size of the existence domains for different numbers of active elements, which was described in the previous section and

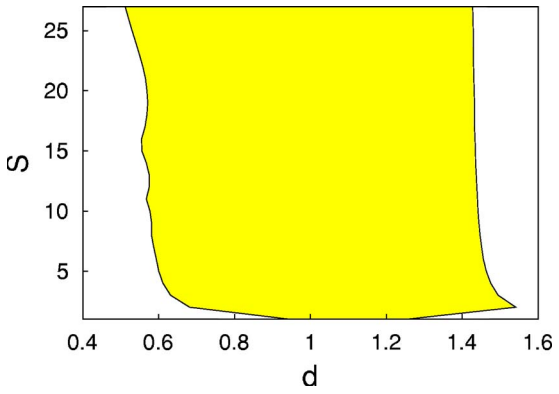

FIG. 13. (Color online) The domain of existence of the cluster mode in which the active cluster consists of 1 element.

shown in Fig. 2. In contrast to that, the upper boundaries of the domains at $S=2$ are very close to each other. As a result, at $S=2$, the domains for modes with different number of active elements are almost the same. We note that a common feature of all these diagrams is that the cluster modes do not exist in the case of local coupling $S=1$, even though they have a significant existence domain at $S=2$, which is approximately $0.74 \lesssim d \lesssim 0.88$ for all of them.

Analyzing the diagrams, we come to a conclusion that the cluster mode with the minimal number of active elements $M=1$ is most probable for local coupling $S=1$. The existence domain of this mode is plotted in Fig. 13. The lower boundary of this existence domain almost coincides with the boundary of the stability domain for the homogeneous passive mode. By contrast, the dependence of the upper boundary is very distinct from what we saw in all previous diagrams: The boundary is almost independent of the range of coupling when $S \geqslant 5$ and corresponds to $d \approx 1.43$. If the range of coupling decreases below this value, the coupling coefficient corresponding to the upper boundary gradually increases up to $d \approx 1.54$, but in the transition from $S=2$ to $S=1$, the boundary shifts abruptly to $d \approx 1.26$. Thus, the sharpest change of the existence domain for this cluster mode occurs in the transition between $S=1$ and $S=2$.

V. CONCLUSIONS

In this paper, we investigated the influence of connectivity on the dynamics in an ensemble of nonlinearly nondiffusively coupled chaotic elements. First, we analyzed the case of global coupling. Unlike more common situations where coupling leads to synchronization of oscillations, the nondiffusive coupling studied here leads to the suppression of oscillations in the whole ensemble when the coupling parameter is sufficiently high. We discovered a novel scenario of transition from the high-dimensional chaos at a low coupling strength to the stationary state at a high coupling strength. A distinct feature of this transition from other cases when there is a partially ordered phase with a large number of coexisting clusters, is that here a two-cluster mode emerges abruptly, replacing the asynchronous mode. We call one of the clusters active and the other passive based on the great difference in their amplitudes. However, the system remains chaotic in time after this transition. Further regularization of the dynamics occurs via the reverse Feigenbaum scheme. Once the coupling strength exceeds the upper boundary of the existence domain for this mode, the number of elements in the passive cluster grows due to a transition to another cluster mode. This gradual growth of the passive cluster eventually leads to the collapse of oscillations and emergence of the homogeneous passive mode. This scenario allows us to view the two-cluster modes as a state of partial suppression of oscillations and give an intuitive explanation of why the number of clusters does not exceed 2: the system is attracted to the full synchronization mode (no synchronous clusters), and the only mechanism that leads to the clustering is the partial suppression of oscillations.

We have analyzed the effects of nonlinearity of the coupling function: the smaller parameter γ the closer function $F(x)$ to the linear in the range spanned by the attractor. For the equilibrium state, our analysis shows that, for linear coupling function as well as for any other function with a positive slope, the equilibrium becomes stable first with respect to the perturbations transversal to the invariant manifold of the homogeneous modes. Then it becomes stable with respect to the perturbations inside the manifold. For the coupling function with a negative slope, these bifurcations occur in the reversed order. This effect has been heuristically explained in terms of positive/negative dissipation introduced by coupling into linearized systems inside the manifold and that for the transversal perturbations.

In contrast, the latter explanation does not work for any oscillatory mode, i.e., for a synchronous solution. In particular, the oscillatory (active) mode exists inside the manifold of homogeneous modes in our system for arbitrary small coupling strength, but it may be unstable with respect to the transversal perturbations. Because of this, the homogeneous oscillatory mode is not realized in the ensemble for low γ, i.e., in the case where the coupling function approaches the linear. The same transversal instability restricts the existence domain of this mode for high γ, i.e., when the slope of the coupling function is negative over the major part of the interval spanned by the attractor

For the diffusive coupling, the type of synchronization is very dependent on the sign of the slope of the coupling function. Our research has shown that, in both cases of negative and positive slope of the coupling function, the in-phase synchronization emerges in the considered system when the coupling strength grows over a threshold. This says that, in the case of nondiffusive coupling, a shift and structural changes of the attractor inside the manifold of synchronization play the major role in stabilizing a synchronous solution.

When the range of coupling S decreases, the existence domains of the two-cluster modes shrink. There is a well-pronounced pattern in this dependence of the domains on S: when the latter decreases, the lower boundaries of the domains shift weakly first, then undergo a quick transition to a higher coupling strength, and stay approximately at that value until $S=2$. For a larger size of the active cluster, the quick transition starts at a higher S and become steeper, occupying the whole range of S. We distinguish a common feature of our diagrams: almost no cluster mode exists in the

case of local coupling, $S=1$. But, by contrast, all of these modes have significant existence domains at $S=2$. This means that the boundaries of the existence domains undergo a very sharp transition when S varies between 2 and 1. This result is also supported by our analytic calculations of the stability boundary for the homogeneous passive mode (stationary state), which shows the most significant shift when S varies in the above interval. Thus, the most significant changes in the dynamics occur in the case of local coupling, when extra connections are added. By contrast, if the number of connections is high, even substantial changes in this number have a much weaker influence on the dynamics.

In the case of global coupling, our research has shown that the dynamics and parametric portraits do not depend on the number of elements N if this number is high. First, the reduced system describing behavior on the manifold of the homogeneous modes does not depend on N. Stability of a solution on this manifold with respect to the transversal perturbations also becomes independent on N for large N. Next, for the two-cluster modes the reduced system depends on the proportion of the active and passive elements, including the ratio M/N, but not the number of elements alone. Finally, the systems for the transversal perturbations in two-cluster modes are the same as in the homogeneous case, but driven by the system on a corresponding manifold. These arguments imply that our results on existence and stability of the cluster modes obtained for $N=55$ can be extended for any other high number of elements. In particular, the existence domains and dynamics in the two-cluster modes must be independent of N if the ensemble remains big. By contrast, in our simulations, we were unable to achieve a mode with a higher number of clusters for $N=55$. Writhing the reduced system and the system for the transversal Lyapunov exponents for any of the latter modes, we can state again that they are independent of the number of elements N. Thus, the cluster modes where the number of clusters is more than two do not exist for any high number of elements.

For changing coupling range, the stability boundary for the equilibrium state is independent of the number of elements, as this follows from our analysis. In the case of more complex modes, such an analytical study is problematic. The investigation of the influence of the population size on the number of clusters is much more complicated as well because the spatial arrangement interferes into the dynamical aspects. Nevertheless, we have shown that all elements can still be identified as active or passive. Inside each of these groups, all dynamical characteristics of the elements are very similar, which allows us to think about these groups as the active and passive clusters. Hence, we apply the definition of a cluster similar to the globally coupled case, neglecting the spatial arrangement. Our simulations have shown that, with this definition we always have at most two well separated clusters. We have tested our results in simulations with an order of magnitude bigger populations (N up to 550) and found qualitatively the same behavior. Nevertheless, we think that computer simulations alone cannot exclude the possibility of existence of more complex solutions. Hence, we focus on a particular class of solutions and note that all our simulations resulted with a solution from this class.

The model studied here emphasizes the important point that the specific nature and the range of coupling may affect drastically the dynamics of large ensembles of elements. We believe that the novel regularization scenario observed in this system can also be observed in other chaotic systems with nonlinear nondiffusive coupling, and this is supported by our previous study [34]. In particular, the same coupling introduced in Ref. [34] in an ensemble of Rössler oscillators also leads to suppression of oscillations which is accompanied by cluster formation, and the number of clusters in that system also undergo an abrupt transition from equal to the number of elements in the range of small coupling strength to a few (3–7) when the coupling strength is above a synchronization threshold. Here we only considered one-dimensional circular arrays of oscillators. Other more complex types of network topology may present additional interesting dynamical features.

ACKNOWLEDGMENTS

This work was partially supported by the Cariplo Foundation for Scientific Research and the Russian Foundation for Basic Research, Grant No. 02-02-17573 (V.S.), by the office of Basic Energy Sciences, U.S. Dept. of Energy, Grant No. DE-DE-FG02-04ER46135 (L.T.), and by NSF Grant No. DMS-0109427 (A.K.). The funding from NATO Collaborative Linkage Grant No. PST.CLG.978512 is gratefully acknowledged.

APPENDIX: THE SYSTEM FOR THE TRANSVERSAL PERTURBATIONS

The transversal perturbations define as ξ, η, ζ such that $x_i=x(t)+\xi$, $x_j=x(t)-\xi$; $y_i=y(t)+\eta$, $y_j=y(t)-\eta$; $z_i=z(t)+\zeta$, $z_j=z(t)-\zeta$, where i and j are the numbers of any two elements from the same cluster (the only cluster), and $x(t), y(t), z(t)$ is a solution on the manifold of a cluster mode (the homogeneous modes). We plug the variables in this form into the systems for ith and jth elements, linearize them and subtract from each other. The resulting system is

$$\frac{d\xi}{dt} = \alpha\{\eta - \xi + f_x'[x(t)]\xi\} - \frac{d}{N-1}F_x'[x(t)]\xi,$$

$$\frac{d\eta}{dt} = \xi - \eta + \zeta,$$

$$\frac{d\zeta}{dt} = -\beta\eta. \tag{A1}$$

Obviously, the coupling term in the first equation is absent if $F_x'[x(t)]=0$, and negligible if the number of elements N is large. In these cases, this system coincides with the linearized system for the isolated element (1). As was indicated above, Eq. (A1) is the same for transversal perturbations in a cluster or homogeneous mode, and the only difference is the system that drives Eq. (A1) via $x(t)$.

[1] A. Pikovsky, M. Rosenblum, and J. Kurths, *Synchronization: A Universal Concept in Nonlinear Sciences* (Cambridge University Press, Cambridge, UK, 2001).
[2] P. C. Matthews and S. H. Strogatz, Phys. Rev. Lett. **65**, 1701 (1990).
[3] V. Hakim and W. J. Rappel, Phys. Rev. A **46**, R7347 (1992).
[4] N. Nakagawa and Y. Kuramoto, Prog. Theor. Phys. **89**, 313 (1993).
[5] N. Nakagawa and Y. Kuramoto, Physica D **75**, 74 (1994).
[6] N. Nakagawa and Y. Kuramoto, Physica D **80**, 307 (1995).
[7] K. Kaneko, Physica D **41**, 137 (1990).
[8] D. H. Zanette and A. S. Mikhailov, Phys. Rev. E **57**, 276 (1998).
[9] M. Rabinovich, J. J. Torres, P. Varona, R. Huerta, and P. Weidman, Phys. Rev. E **60**, R1130 (1999).
[10] W. Wang, I. Z. Kiss, and J. L. Hudson, Chaos **10**, 248 (2000).
[11] C. van Vreeswijk, Phys. Rev. E **54**, 5522 (1996).
[12] K. Okuda, Physica D **63**, 424 (1993).
[13] A. Crisanti, M. Falcioni, and A. Vulpiani, Phys. Rev. Lett. **76**, 612 (1996).
[14] I. Z. Kiss, Y. Zhai, and J. L. Hudson, Phys. Rev. Lett. **88**, 238301 (2002).
[15] J. L. Rogers and L. T. Wille, Phys. Rev. E **54**, R2193 (1996).
[16] S. E. de S. Pinto and R. L. Viana, Phys. Rev. E **61**, 5154 (2000).
[17] L. S. Tsimring, N. F. Rulkov, M. L. Larsen, and M. Gabbay, Phys. Rev. Lett. **95**, 014101 (2005).
[18] M. Marodi, F. dOvidio, and T. Vicsek, Phys. Rev. E **66**, 011109 (2002).
[19] C. Anteneodo, S. E. de S. Pinto, A. M. Batista, and R. L. Viana, Phys. Rev. E **68**, 045202(R) (2003).
[20] A. Zumdieck, M. Timme, T. Geisel, and F. Wolf, Phys. Rev. Lett. **93**, 244103 (2004).
[21] S. C. Manrubia and A. S. Mikhailov, Phys. Rev. E **60**, 1579 (1999).
[22] P. J. Kim, T. W. Ko, H. Jeong, and H. T. Moon, Phys. Rev. E **70**, 065201(R) (2004).
[23] V. S. Afraimovich, V. I. Nekorkin, G. V. Osipov, and V. D. Shalfeev, *Structures and Chaos in Nonlinear Synchronization Networks* (World Scientific, Singapore, 1995).
[24] W. S. Lindsey, *Synchronization Systems in Communication and Control* (Prentice-Hall, Englewood Cliffs, NJ, 1972).
[25] D. J. Sturzebecher, X. Zhou, X. Zhang, and A. S. Daryoush, IEEE Trans. Microwave Theory Tech. **41**, 998 (1993).
[26] D. R. Stephens, *Phase-locked Loops for Wireless Communications: Digital, Analog, and Optical Implementations* (Kluwer Academic, Boston, MA, 2002).
[27] A. Djemouai, M. A. Sawan, and M. Slamani, IEEE Trans. Circuits Syst., II: Analog Digital Signal Process. **48**, 441 (2001).
[28] T. Stace, A. N. Luiten, and R. P. Kovacich, Meas. Sci. Technol. **9**, 1635 (1998).
[29] E. A. Gerber and A. Ballato, *Precision Frequency Control* (Academic Press, Orlando, FL, 1985).
[30] M. S. Fee, S. Chu, A. P. Mills, R. J. Chichester, D. M. Zuckerman, E. D. Shaw, and K. Danzmann, Phys. Rev. A **48**, 192 (1993).
[31] P. Dayan and L. Abbott, *Theoretical Neuroscience. Computational and Mathematical Modeling of Neural Systems* (MIT Press, Cambridge, MA, 2001).
[32] A. S. Kuznetsov and V. D. Shalfeev, *Cellular Neural Networks and their Applications, 2000*, Proceedings of the 2000 6th IEEE International Workshop (Catania, Italy, 2000) p. 419.
[33] *Chua's Circuit: A Paradigm for Chaos*, edited by R. Madan (World Scientific, Singapore, 1993).
[34] A. S. Kuznetsov and J. Kurths, Phys. Rev. E **66**, 026201 (2002).